

Received 18 April 2024, accepted 4 May 2024, date of publication 15 May 2024, date of current version 29 May 2024.

Digital Object Identifier 10.1109/ACCESS.2024.3401651

## RESEARCH ARTICLE

# Low-Cost LIDAR-Based Monitoring System for Fall Detection

MIGUEL PIÑEIRO<sup>1</sup>, DAVID ARAYA<sup>1</sup>, DAVID RUETE<sup>1</sup>, AND CARLA TARAMASCO<sup>1,2</sup>

<sup>1</sup>Instituto de Tecnología e Innovación para la Salud y Bienestar, Facultad de Ingeniería, Universidad Andrés Bello, Viña del Mar 2531015, Chile

<sup>2</sup>Núcleo Milenio de Sociomedicina, Viña del Mar 2530959, Chile

Corresponding author: Miguel Piñeiro (miguel.andres.pineiro.feick@gmail.com)

This work was supported in part by the FONDECYT Regular Project “Multimodal Machine Learning Approach for Detecting Pathological Activity Patterns in Elderlies” under Grant 1201787, in part by the FOVI220145 Project “International Collaboration Program for Research and Development of Intelligent Environments,” and in part by STIC-AmSud under Grant 230045.

**ABSTRACT** Every year, over 30% of individuals aged 65 and above experience fall, leading to potential physical and psychological harm. This is particularly concerning for those who live independently and lack immediate assistance. To address this issue, numerous studies in the field have focused on early fall detection of the elderly, employing diverse sensors and algorithms. In this paper, we present a low-cost fall detection system based on Laser Imaging, Detection And Ranging (LIDAR) technology, specifically designed for older individuals residing alone, monitoring daily routines without disruption and without camera, to respect user privacy, as these are essential factors for user acceptance and overall effectiveness. The system’s significance lies in its capacity to function with minimal computational resources and its high level of interpretability. This is due to our solution being based on Finite State Machines (FSM), which contain clear rules, distinguishing between different states such as no human presence, human presence, and a fall, offering a more transparent and interpretable detection process. These characteristics contrast with traditional methods such as Support Vector Machine (SVM) and Artificial Neural Network (ANN), which are more computationally expensive and operate as black boxes. This approach combines simplicity, low computational load, privacy preservation, low cost, interpretability, and high accuracy. It represents an advancement in enhancing the care and safety of older adults living independently.

**INDEX TERMS** Fall detection, older people, finite state machines, LIDAR technology.

## I. INTRODUCTION

The rapid aging of the global population is fueled by a decrease of fertility rates and rising life expectancy. The share of the global population aged 65 years or above is projected to rise from 10% in 2022 to 16% in 2050 [1], significantly affecting healthcare and social service planning [2]. The global fertility rate dropped to 2.3 children per woman in 2023, a sharp decrease from about 5 in 1950, showing that women are now having less than half as many children as they did seventy years ago [3]. This demographic transition, with declining birth rates and longer lifespans, is causing a marked increase in the older adult population segment.

The associate editor coordinating the review of this manuscript and approving it for publication was Joewono Widjaja.

Falls among older adults represent a major healthcare challenge due to their high frequency and potentially severe outcomes. Research reveals that about 30% of individuals aged 65 and older experience falls annually. These falls significantly affect their quality of life and place a considerable strain on healthcare systems [4], [5], [6]. The repercussions of these falls range from physical injuries to psychological impacts, leading to increased healthcare costs and the need for long-term care. Early and precise detection of falls is essential in reducing these risks. Early and precise detection of falls is essential in reducing the risks associated with delayed medical attention and prolonged immobility, which can lead to several health complications.

To tackle the challenge of falls in older adults, a range of tools and techniques are being investigated. This includes wearable devices and context-aware systems [7], [8] along

with advanced technologies such as computer vision [9], [10] and machine learning [11], [12]. Each method has its own benefits and drawbacks, including issues of user acceptance, technical complexity, and privacy concerns. Developing effective fall detection solutions is vital for enhancing the safety and independence of the elderly, a goal that remains a focus in this evolving field of research.

In addressing falls among older adults, innovative detection methods are key. Ground vibrations have been explored as a non-intrusive technique for distinguishing fall types, especially useful in scenarios where wearables or cameras are impractical [13]. Crucial also is data analysis and interpretation, where advanced processing and predictive analytics identify patterns to preempt falls, aiding in effective preventive measures [14], [15]. Emerging research focuses on real-time alert systems, notifying caregivers or medical services post-fall, crucial for timely intervention. Ergonomic design in wearable technologies ensures user comfort and acceptance, vital among older adults who might resist new technology. Interdisciplinary collaboration among engineers, medical professionals, designers, and ethicists is fundamental, balancing technical functionality with user needs. This evolving field, merging technology and public health, highlights the need for adaptable, integrated solutions for older adults.

Research on fall detection has made significant progress, mainly through the use of machine learning algorithms [16]. These algorithms share methods and technologies with applications in seemingly distant fields, such as anomaly and fault detection in engines and machinery. In both cases, discriminating between normal and abnormal situations using data about a basal training while continuously adjusting to new data is a significant challenge for the algorithm, named “universal source-free domain adaptation”.

Despite current advancements, the most significant challenge is to develop technologies that are not only effective but also non-intrusive, that do not infringe on privacy or disrupt user’s daily routines, thus ensuring their autonomy and dignity [17]. It is vital for older adults to make decisions based on their personal preferences and environmental needs, thereby maintaining their independent lifestyle. Consequently, it is very important that fall detection methods be non-portable and as unobtrusive as possible, avoiding devices that might be uncomfortable or rejected [18]. While options like thermal cameras [19] and vibration sensors [13] are viable, each has its limitations, such as the high cost of thermal cameras [20] and the limitations of vibration sensors, which most proposed systems tend to use high-sensitivity sensors that are too expensive for widespread use in senior housing [13].

Furthermore, the challenges faced by artificial intelligence (AI) algorithms in fall detection include the complexity of the algorithms, the opacity of “black box” models [21], [22], and the need for extensive datasets [4], [5], [6]. These challenges often require large amounts of data and intensive parameter tuning, which increase computational costs and limit their

applicability in diverse environments [23], [24]. To address these challenges, we suggest a solution that employs low-cost 3D LIDAR technology [25] with a computationally efficient and explainable Finite State Machine (FSM) algorithm.

LIDAR (Light Detection and Ranging) is an optical scanning technology that obtains distance information from an object [26]. LIDAR technologies vary by scanning method, leading to three common types: Mechanical Scanning, Solid-State, and Flash. Mechanical Scanning LIDARs use rotating laser detectors to cover a wide area, providing detailed 360° point clouds. Solid-State LIDARs employ either MEMS (Micro-Electromechanical Systems) or OPA (Optical Phased Arrays) to steer laser beams without moving parts, offering more durability and safety. Flash LIDARs operate similarly to a camera’s flash, illuminating the entire scene at once to create a point cloud, suitable for close-range applications due to their lower resolution and range. LIDAR technology can also be categorized into 2D and 3D systems based on the dimensional data they produce. 2D LIDAR sensors scan the environment in a single plane, offering valuable data for flat surface mapping and basic obstacle detection. In contrast, 3D LIDAR systems provide a three-dimensional view of the surroundings, capturing detailed shapes and the spatial relationship of objects, making them ideal for complex environment mapping and advanced navigation tasks.

It was historically known that LIDAR technology is expensive and power-demanding [27], and was initially utilized in specialized fields such as meteorology, agriculture, and autonomous driving [28], [29]. However, significant advancements have made LIDAR more affordable, smaller, and energy-efficient [30], [31]. Consequently, LIDAR technology has expanded its applications to include human identification [32], tracking in public spaces [33], [34], activity recognition [35], [36] and fall detection [25], [37], [38]. Regarding these last two applications, it is important to note that since LIDAR flash type captures data as 3D point clouds, it inherently preserves privacy by avoiding personal information, unlike camera-based systems. Its deployment in fall detection systems ensures that the elderly’s daily comfort is not compromised. This is due to its non-intrusive setup, which simply requires positioning the device in a strategic location for comprehensive monitoring. This solution not only overcomes precision and privacy limitations but is also distinguished by its low computational load and ease of interpretation. Regarding safety, the use of Class 1 lasers in LIDAR systems, as defined by IEC standards, ensures that the laser exposure is safe for human eyes, even under prolonged use.

The article is organized as follows: Section II summarizes the work already developed in this area of study and the contribution of each one of these works. Section III details the methodology used, such as the implemented system and the algorithms used in the processing of information, the test environment, sensor characterization, and the dataset used. Section IV shows the results obtained in the classification

of falls, and Section V delivers the discussion of the results. Finally, conclusions and future work are presented in Section VI.

## II. RELATED WORK AND CONTRIBUTION

In the field of fall detection, there is a wide range of solutions that vary based on the technology used, the AI algorithms employed, and whether they are intrusive or non-intrusive, among other aspects [39], [40]. This latter classification is particularly relevant for our analysis. In the category of intrusive solutions for fall detection, there are studies that analyzed acceleration signals from an inertial sensor placed on the lower back during 143 real-world falls with a sensitivity over 80% and false alarm rate of 0.56 per hour [4]. A study comparing various machine learning algorithms revealed that the random forest model achieved an accuracy of 99.2% [5]. Using a perturbation treadmill for simulated falls, a study demonstrated that the DeepConvLSTM model achieved an F1 score of 0.954 [6]. One study utilized various algorithms to achieve up to 97.7% accuracy, while another research effort led to the design of a sock-based electronic textile device that differentiated falls with up to 99.4% accuracy using a Bidirectional Long Short-Term Memory (Bi-LSTM) network [7], [41]. Wearable sensors and machine learning were utilized for fall risk prediction, achieving an accuracy of 78.5% [42]. Wearable devices with a triaxial accelerometer were tested, with one-class SVM showing the best results for forward falls [23]. A system using K-Nearest Neighbors (KNN) for fall detection achieved an accuracy of 99.8% [24]. An analysis of wrist-worn device data revealed that neural networks and random forest algorithms achieved an accuracy of over 90% [43]. FallDroid, a smartphone-based system based demonstrated high accuracy and sensitivity [44]. A video stream fall detection algorithm was introduced, achieving an accuracy of 0.92% [9], while another approach using a convolutional and spatiotemporal attention neural network achieved up to 99.93% accuracy [11]. Rapid pose estimation was utilized for fall detection in a study [10], and computer vision and machine learning were applied to achieve a 98.2% accuracy in detecting falls without the use of sensors [12]. These cases are successful and provide a good solution for preventing and detecting falls; however, they are intrusive solutions, which have the end user as a risk factor for success.

In the realm of non-intrusive fall detection, various innovative technologies have been explored. A study utilized low-resolution infrared sensor arrays with a resolution of  $16 \times 16$  pixels, applying Multilayer Perceptron (MLP) neural networks for classification [45]. Despite limited success due to their training set, these sensors were favored for their privacy advantages over traditional camera-based systems, highlighting the importance of user acceptance in the development of such technologies. In a related study, researchers implemented two low-resolution sensor arrays on a wall and ceiling. Their system, designed to estimate body posture for fall detection through posture changes, achieved

an accuracy of 72.7% in worst-case scenarios [46]. This indicates the potential of sensor arrays in effectively monitoring movements without compromising privacy. The application of various deep learning methods, including LSTM and Gated Recurrent Unit (GRU), to  $8 \times 8$  pixel infrared sensor arrays was explored [47]. Their findings showed promising results, with accuracies of 75% for the GRU with attention (GRUAtt) algorithm and 85% for Long Short-Term Memory (LSTM) networks, suggesting the efficacy of deep learning techniques in interpreting data from low-resolution sensors for fall detection. Recurrent neural networks with a convolutional layer were utilized on  $16 \times 2$  pixel infrared sensors, as demonstrated in [2]. The focus here was on safeguarding user privacy while accurately detecting falls. Their innovative approach employed four  $1 \times 8$  pixel sensors placed at different heights to cover a wider area, successfully integrating multiple data points for a more comprehensive fall detection system. This study underscores the importance of sensor placement and data integration in designing effective fall detection systems. Another approach using the eHomeSeniors dataset is employing two different infrared thermal sensors that respect user privacy [19]. This dataset, constructed by volunteers including young individuals and performing artists, offers a unique resource for developing and testing fall detection systems. Using WiFi Channel State Information (CSI) for fall detection was proposed, and its potential was evaluated with a comprehensive dataset, as suggested [48]. Their deep learning-based classifier, applied to data from four different indoor settings, achieved an accuracy exceeding 96%, demonstrating the feasibility of using existing network infrastructure for fall detection. The use of millimeter-wave radar technology (mmWave) for discreet fall detection was implemented [49]. By collecting data with the radar mounted in different positions in an experimental room, they applied various classifiers, including MLP, Random Forest (RF), KNN, SVM, and Convolutional Neural Network (CNN). The RF and CNN models achieved accuracies of over 92%, showcasing the potential of mmWave technology in detecting human falls without the need for wearable devices. A classification framework using ground vibrations was proposed, involving a novel approach that simulated human body movement to generate fall data [13]. Employing K-means and KNN classifiers, they achieved accuracies of 85% and 91%, highlighting the potential of ground vibration sensors in differentiating fall events and postures. These studies demonstrate the potential of non-intrusive technologies in fall detection, highlighting advances in sensor technology, machine learning, and the importance of privacy in designing systems for the elderly. However, challenges such as implementation costs, computational expenses, the complexity of algorithms, and the amount of data required to feed these models are still present.

AI in fall detection faces challenges such as complex algorithms, the opacity of “black box” models, and the need for extensive datasets. Advancements in machine learning for fall detection, as shown in various studies, often necessitate

large datasets and extensive feature engineering to achieve accurate results [4], [5], [6]. The use of SVM and ANN [7], [41] presents interpretation challenges due to their “black box” nature. Practical implementation of these systems, raises feasibility and adaptability questions [8], [42]. The extensive data needed may limit their applicability in diverse environments [23], [24]. In non-intrusive scenarios, balancing privacy and effectiveness is crucial [45], [46]. Recurrent neural networks and low-cost sensors offer promise but require more practical, user-friendly adaptations [2], [48]. Future research should focus on improving accuracy, reducing false positives, and enhancing transparency for better user adoption [13], [19], [49].

Our research is focused on developing an affordable and non-intrusive fall detection system that protects the privacy of elderly individuals living independently. To achieve this, we have chosen to base our system on a low-cost, low-resolution solid-state LIDAR sensor [25] and use memory-efficient and computationally lightweight algorithms that can operate on inexpensive microcontrollers. These are based on a FSM with predefined thresholds set by simple functions, providing a more effective and understandable solution in certain contexts, such as fall detection, compared to more complex AI based systems. The FSM is inherently more explicable due to its transparent and predictable structure. Each state is clearly defined, and transitions between states occur according to specific and easily understood rules. This contrasts with AI models that often function as “black boxes”, where internal processes and decision-making are not easily interpretable by end-users. Additionally, there is a noticeable reduction in implementation and maintenance costs. They do not require the same amount of data or the complex feature engineering needed for machine learning models. The predefined thresholds in an FSM can be based on simple functions and logical rules, significantly reducing development and computing costs. In applications such as fall detection, where speed and reliability of response are crucial, our solution provides quick and reliable results. Its simplicity allows for rapid identification of critical events, such as a fall, with fewer possibilities of errors and greater ease in making adjustments and improvements. The clarity and economy of our proposal make it particularly suitable for applications in environments where resources are limited and explainability and scalability are essential.

### III. METHODOLOGY

#### A. SYSTEM ARCHITECTURE

The system includes a LIDAR board connected to a microcontroller board through I<sup>2</sup>C. The microcontroller connects to the computer through a USB virtual serial port and acts as an intermediary between the LIDAR sensor and the computer. More specifically, the microcontroller initially configures the LIDAR and subsequently transmits the raw LIDAR data it captures to the computer in real-time. On the computer side,

a Python program receives the incoming data, archives it for subsequent analysis, and processes it accordingly (Figure 1).

#### B. HARDWARE

In our LIDAR-based fall-detection setup, we utilized the ST VL53L5CX-SATEL<sup>1</sup> breakout board, which features an ST VL53L5CX<sup>2</sup> sensor module. This sensor is implemented within a compact  $6.4 \times 3.0 \times 1.5$  mm chip and employs a 940 nm vertical cavity surface emitting laser (VCSEL). It offers a maximum range of 4 meters, encompassing a square Field Of View (FOV) of  $45^\circ \times 45^\circ$ , with a maximum resolution of  $8 \times 8$  and a maximum sampling frequency of 60 Hz. The selection of this specific integrated circuit (IC) was based on its cost-effectiveness, priced at approximately 5.1 USD for quantities of 1000 units and 9.1 USD for individual units.

A key consideration when configuring the system is the trade-off between sampling rate and measurement accuracy. Higher sampling rates are associated with a greater likelihood of obtaining less accurate measurements or, in some cases, failing to obtain measurements altogether. Conversely, lower sampling rates yield more reliable measurements but may pose challenges in detecting falls. We chose a 10 Hz sampling rate, striking a balance that ensures significant accuracy without compromising the sampling rate to an extent that would hinder fall detection.

As microcontroller we used a board with an Espressif ESP32<sup>3</sup> and a Silicon Labs CP2102<sup>4</sup> USB-UART bridge. This choice was primarily driven by cost-effectiveness and ease of programmability. The selected microcontroller possessed sufficient memory and computation capabilities for the intermediary role and, if required, it could also support the implementation of the fall detection algorithm.

Following the initialization of the LIDAR sensor, the microcontroller continuously transmits the LIDAR data in CSV format through an USB virtual serial port configured at a rate of 921,600 bits per second (bps) to the computer.

The primary reason for choosing the CSV format is its inherent simplicity. This simplicity eases the implementation process on the microcontroller and facilitates data parsing through Python libraries. Additionally, the data transmission rate observed during our experiments, roughly 13,700 bps is significantly lower than the capacity of our virtual serial port link (921,600 bps). While a binary format might enhance transmission efficiency, it would complicate the implementation of the data encoder and decoder unnecessarily.

The LIDAR sensor and microcontroller board were mounted on the ceiling at a height of 2.7 m, with its orientation directed vertically downward toward the floor (Figure 1).

<sup>1</sup><https://www.st.com/en/evaluation-tools/vl53l5cx-satel.html>

<sup>2</sup><https://www.st.com/en/imaging-and-photonics-solutions/vl53l5cx.html>

<sup>3</sup><https://www.espressif.com/en/products/socs/esp32>

<sup>4</sup><https://www.silabs.com/interface/usb-bridges/classic/device.cp2102>

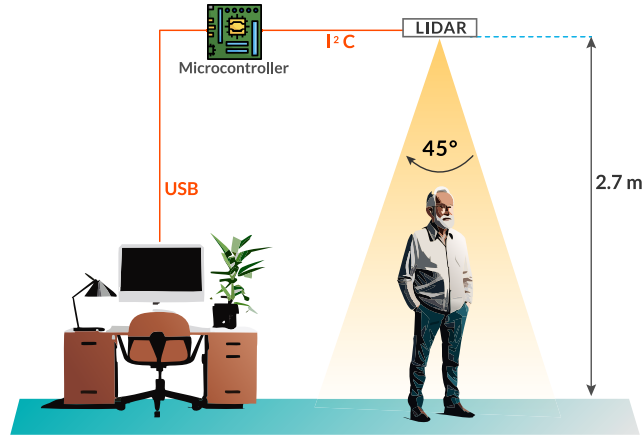


**FIGURE 1.** LIDAR data acquisition setup. A LIDAR sensor mounted on the ceiling of a room, facing downward, scans the activity within its field of view.

### C. DATA ACQUISITION

To assess, fine-tune, and evaluate fall detection algorithms, we generated two datasets: one of falls and one of non-fall activities. For the fall activity dataset, six subjects participated to simulate three distinct types of falls each. The experimental protocol involved a phase where participants walked around the visual field of the LIDAR, followed by the simulation of three fall scenarios: tripping, collapsing, and falling while attempting to stand up from a seated position. After each fall, a simulation of a 10-second period of inability to stand up was included. For the non-fall activities dataset, three subjects participated to simulate a variety of non-fall activities, including sitting on a chair, sitting on the floor, picking up a wallet from the floor, and tying their shoes.

A total of six healthy male participants, aged between 32 and 45, with heights ranging from 1.7 to 1.94 m and weights ranging from 65 to 105 Kg, were involved in generating the dataset.

### D. ALGORITHM

#### 1) FINITE STATE MACHINE TRANSITION DIAGRAM

The algorithm operates as a FSM with five distinct states: NO\_HUMAN, HUMAN, FALL, ALERT, and ON\_FLOOR (Figure 2). There are three conditions that can lead to a transition between states: The `human()` function returning True, the `activity()` function returning False, or the FALL state timing out. The explanation of the parameters passed to these functions will be provided at a later point.

The FSM begins in the NO\_HUMAN state and transitions to the HUMAN state upon detecting human presence. When in the HUMAN state, it can either revert to the NO\_HUMAN state if it no longer detects human presence or shift to the FALL state if a fall is detected. In the FALL state, it can return to the HUMAN state upon detecting a person standing or progress to the ALERT state if it cannot detect a standing person before a specified timeout elapses or if no activity is detected after entering the FALL state (i.e: the person is

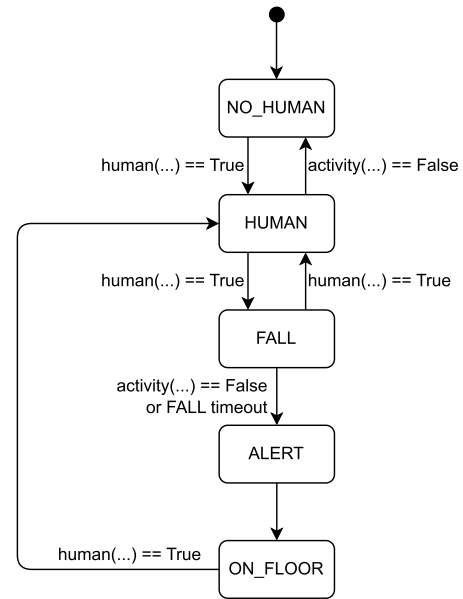


**FIGURE 2.** Finite state machine diagram.

unconscious on the floor). The ALERT state is where an alert can be generated and sent to the responsible caregiver before transitioning to the ON\_FLOOR state. At the ON\_FLOOR state it will only transition to the HUMAN state upon detecting a standing human.

Detecting falls poses a unique challenge due to two specific characteristics of the LIDAR mode of operation. The first challenge arises from the frequent absence of distance measurements at certain cells of the matrix, visualized as a black cell, which depend on the surface's distance from the LIDAR and its reflectivity (Figure 3). The second challenge involves instances where the LIDAR may occasionally provide significantly different distance measurements for the same surface, with variations observed in our experiments of up to 0.5 m.

#### 2) ACTIVITY DETECTION TRANSITION CONDITION

The `activity()` function evaluates whether the activity detected by the LIDAR surpasses a predefined threshold. It requires two parameters: a time window length and an activity threshold.

The function computes the average difference between the most recent distance matrix and each preceding distance matrix within the specified time window. Subsequently, it calculates the mean of these averages and compares it to a predefined threshold. Mathematically the function can be expressed as follows:

$$V_{ij}(M) = \begin{cases} 1, & \text{if } M_{ij} \neq 0 \\ 0, & \text{otherwise} \end{cases}$$

$$W_{ij}(M) = V_{1ij}(M)V_{2ij}(M)$$

$$w_t(M) = \sum_{i=1}^8 \sum_{j=1}^8 W_{ij}(M)$$

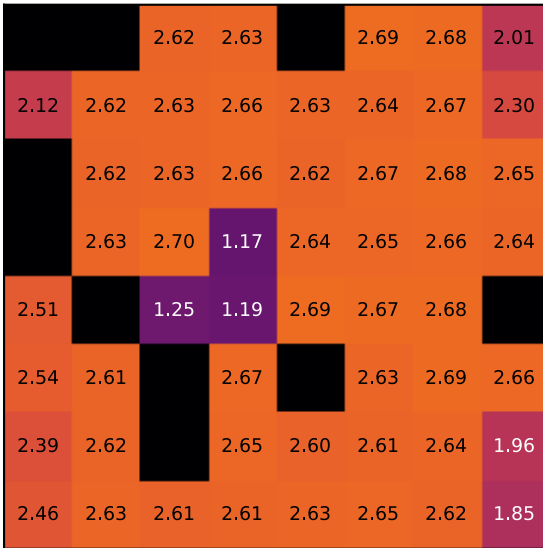


**FIGURE 3.** LIDAR distance matrix sample. Top displays the test room with a person positioned within the LIDAR’s field of view. Bottom shows the corresponding distance matrix captured by the LIDAR. Distance are expressed in meters and black elements indicate instances where the LIDAR was unable to measure at that particular location.

$$s(M, t_{\max}) = \frac{1}{t_{\max} - 1} \sum_{t=2}^{t_{\max}} \frac{1}{w_t(M)} \sum_{i=1}^8 \sum_{j=1}^8 |M_{1ij} - M_{tij}| W_{ij}(M)$$

$$a(t_{\max}, k) = \begin{cases} 1, & \text{if } s(D, t_{\max}) > k \\ 0, & \text{otherwise} \end{cases}$$

where:

- $W_{ij}$  is a function that returns a tensor with elements equal to 1 where the subtraction of the most recent matrix and the matrix at time  $t$  gives a valid result, or 0 otherwise.
- $w_t$  is a vector that specifies the total number of valid elements of the subtraction of the most recent matrix and the matrix at time  $t$ .
- $s$  is a function that returns the mean difference between the most recent matrix and the preceding  $t_{\max} - 1$  matrices.
- $a$  is the `activity()` function and returns 1 if the LIDAR distance matrix activity during the most

recent  $t_{\max}$  captures surpasses a specified threshold, or 0 otherwise.

- $D$  represents the distance between the ceiling and the object where the laser beam reflects. A value of 0 indicates that at the corresponding position, the LIDAR could not measure the distance.

### 3) HUMAN DETECTION TRANSITION CONDITION

The `human()` function can detect the presence of a human in various positions such as standing, sitting, or on the floor. The function requires 5 parameters: the minimum distance difference to distinguish the background from the foreground (e.g., humans), the minimum and maximum distances at which the LIDAR should detect the human, a threshold for the minimum number of elements of a blob, a time window length for the blob, and an activity threshold for the blob.

An additional challenge in the deployment of fall detection systems is the presence of pets or other moving objects, which can potentially trigger false alarms. Our system employs height discrimination algorithms, which utilize the distance data provided by the LIDAR sensor to determine whether the object in motion matches the typical height range of a human. This method effectively reduces false positives caused by pets and other small moving objects within the environment.

The function keeps track of a basal matrix as new distance matrices are received. With each new matrix, the function recalculates the highest distance for each matrix element. This ensures that the basal matrix represents the distance of the static objects in the room (e.g., walls, furniture). Elements from the latest distance matrix that exceed a specified threshold distance from the basal matrix and fall within a defined range of minimum and maximum values are selected to generate a list of blobs. Each blob of the list is then examined to determine if it exceeds a minimum number of elements and exhibits a minimum level of activity within a specified time window. Mathematically, the function can be expressed as follows:

$$X_{ij} = \max_{t \in T} (d_{ij})$$

$$M_{ij} = \begin{cases} D_{1ij} & \text{if } X_{ij} - D_{1ij} \geq h_{\text{diff}} \text{ and } h_{\max} \geq D_{1ij} \geq h_{\min} \\ 0 & \text{otherwise} \end{cases}$$

$$N_{ij} = \begin{cases} 1 & \text{if } M_{ij} \neq 0 \text{ or } D_{1ij} = 0 \\ 0 & \text{otherwise} \end{cases}$$

$$B_{kij} = \begin{cases} 1 & \text{if } (i, j) \in \text{blob-}k \text{ of matrix } N \\ 0 & \text{otherwise} \end{cases}$$

$$e_k = \sum_{i=1}^8 \sum_{j=1}^8 B_{kij} V_{1ij}(D)$$

$$h(h_{\text{diff}}, h_{\min}, h_{\max}, e_{\min}, t_{\max}, a_{\text{blob}})$$

$$= \begin{cases} 1 & \text{if } \exists k \in K \text{ such that} \\ & e_k \geq e_{\min} \text{ and } s(D_{ij} B_{kij}, t_{\max}) \geq a_{\text{blob}} \\ 0 & \text{otherwise} \end{cases}$$

where:

- $X$  is the basal matrix that keeps track of the steady objects of the room.
- $M$  is a matrix that stores the distance value elements of the most recent distance matrix if each of these elements meet two conditions: The distance matrix element must have a minimum separation from the basal matrix specified by threshold and each element of the distance matrix must fall within a minimum and maximum value.
- $N$  is a matrix where elements that can indicate the presence of a human are set to 1, while the remaining elements are set to 0.
- $B$  is the tensor that contains matrices single blobs.
- $e_k$  is a vector with the total number of possible human elements within each blob matrix.
- $h$  is the  $human()$  function and returns 1 if human presence in the most recent distance matrix, that meets the detection parameters, is detected, or 0 otherwise.

#### 4) STATE MACHINE TRANSITION FUNCTION PARAMETERS

The FSM's conditional functions receive a combined total of 14 parameters across three sets. The  $activity()$  function receives one set of 2 parameters, while the  $human()$  function receives two sets of 6 parameters each. One aimed to detect a non-fallen human (e.g., a standing or seated human), and the other set aimed to detect a fallen human.

To evaluate the prediction capability of the algorithm, we visually classified the state of the captured LIDAR data with the help of the video recording. We categorized the state into three distinct categories:  $NO\_HUMAN$ ,  $HUMAN$ , and  $FALL$ . We used the differential evolution global optimization algorithm to maximize the expression  $TP - FP - FN + ACC$ , where  $TP$  represents the true positives,  $FP$  the false positives,  $FN$  the false negatives, and  $ACC$  the accuracy of the prediction.

$TP$ ,  $FP$  and  $FN$  were evaluated at event granularity, while  $ACC$  was evaluated at sample granularity during the optimization of the binary classifier.  $TP$  indicates that during a contiguous actual  $FALL$  state, there is a single transition to an  $ALERT$  state. A second transition within the same event is categorized as a  $FP$ . Transitions to  $ALERT$  outside of  $FALL$  events are also considered  $FP$ . A  $FN$  occurs when during a  $FALL$  event no transition to an  $ALERT$  state occurs. A  $TN$  occurs when during an actual state transition from  $NO\_HUMAN$  to  $HUMAN$  and back to  $NO\_HUMAN$  the FSM does not transition to an  $ALERT$  state.

The rationale behind integrating  $TP$ ,  $FP$ ,  $FN$  and  $ACC$  into the optimization function despite their differing dimensionality stems from their operational levels during the optimization.  $TP$ ,  $FP$ , and  $FN$  operate at fall event granularity, while  $ACC$  operates at sample granularity.

This differentiation in granularity means that adjustments made by the optimizer to the model parameters might lead to changes that do not immediately affect  $TP$ ,  $FP$ , and  $FN$  counts. These metrics might remain unchanged because they depend

on the correct identification of discrete events.  $ACC$ , however, being sensitive to changes at the sample level, can reflect minor adjustments in model parameters more immediately. Therefore, incorporating  $ACC$  into the optimization criterion allows the optimizer to receive feedback and direction for parameter space exploration, even in scenarios where the event-based metric  $TP - FP - FN$ , which is the metrics that we care the most to optimize, remains static.

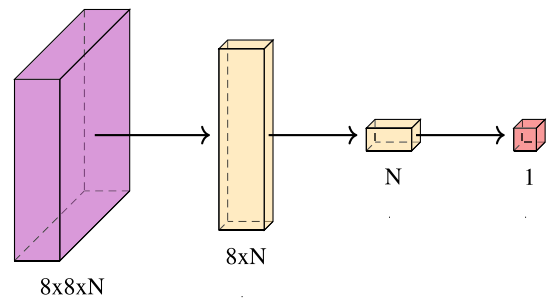


**FIGURE 4.** Neural network architecture. The input LIDAR distance tensor made of  $N$  frames is show in purple, the hidden one-dimensional linear layers in yellow, and the output layer in red.

#### 5) ALTERNATIVE ALGORITHMS

To assess the efficacy of the FSM, we trained SVM and ANN models for comparative analysis of their performance. The SVM models used a Radial basis function (RBF) kernel and were designed to operate with 1, 2, 4, 8, 16, 32, 64 and 128 consecutive LIDAR frames, while the ANN models were designed to operate with 1, 2, 4, 8 and 16 consecutive frames only.

The ANN architecture incorporated linear layers and has its first layer with a number of neurons equal to 8 multiplied by the number of frames used by each particular model (Figure 4). The subsequent layer decreases the neuron count to match the number of frames employed by the specific model. If the model's frame count exceeds one, an additional layer consisting of a single neuron is introduced. To reduce the possibilities of overfitting a 20% dropout layer was added after each hidden layer.

#### 6) TRAINING AND VALIDATION

Given the limited number of participants in our experiments, we split the total recordings into two distinct datasets for training and validation/testing purposes. The training dataset comprised three fall records and two non-fall records, whereas the validation/testing dataset included three fall records and a single non-fall record. We selected the subjects for each dataset to ensure a similar height distribution among participants. The validation/testing dataset was employed to validate the Finite State Machine (FSM) and Artificial Neural Network (ANN) models and to test the SVM model. For training the SVM and ANN models, we considered only two states, which represent the presence or absence of a person on the floor. Unlike the FSM-based algorithm, the SVM

and ANN models were trained with a focus on sample-level granularity.

In order to prevent overfitting of the SVM models, we employed 5-fold cross-validation. The objective was to identify the model with the highest accuracy among various  $C$  regularization parameter values, covering an inclusive range of powers of 2 from 1 to 1024.

**IV. RESULTS**

We optimized the parameters of the FSM to maximize  $TP-FP-FN + ACC$ , resulting in the values presented in Table 1.

**TABLE 1. Optimized parameter values.**

activity () parameters	
$t_{max}$	128
$k$	0.0170
human () parameters to transition to HUMAN state	
$h_{diff}$	0.798
$h_{min}$	0.752
$h_{max}$	1.710
$e_{min}$	2
$t_{max}$	14
$a_{blob}$	0.490
human () parameters to transition to FALL state	
$h_{diff}$	0.094
$h_{min}$	2.101
$h_{max}$	2.399
$e_{min}$	1
$t_{max}$	18
$a_{blob}$	0.267

To assess performance, we calculated the number of TP, FN, TN and FP at event granularity for each subject, along with the respective overall totals (Table 2).

**TABLE 2. Classification performance of the fall detector at event granularity. A-F represent fall records, while NF1-NF3 represent no-fall records.**

Record	TP	FN	TN	FP
A	9	0	23	0
B	9	0	26	1
C	9	0	20	1
NF1	0	0	7	1
NF2	0	0	6	0
D	9	0	20	0
E	9	0	20	1
F	9	0	27	1
NF3	0	0	7	0
Training dataset	27	0	82	3
Validation dataset	27	0	74	2

We then proceeded to assess the true positive rate (TPR), false negative rate (FNR), true negative rate (TNR), false positive rate (FPR) and accuracy (ACC) of the model at sample granularity (Table 3). This allowed us to compare the performance of different models on the validation/testing dataset (Table 5).

To better visualize and compare the models, as well as take advantage of the ability of SVM and ANN models to easily

**TABLE 3. Classification performance of the fall FSM detector at sample granularity.**

Record	TPR	FNR	TNR	FPR	ACC
A	0.907	0.093	0.947	0.053	0.934
B	0.940	0.060	0.890	0.110	0.905
C	0.880	0.120	0.944	0.056	0.925
NF1			0.957	0.043	0.957
NF2			0.986	0.014	0.986
D	0.933	0.067	0.944	0.056	0.941
E	0.958	0.042	0.745	0.255	0.808
F	0.929	0.071	0.894	0.106	0.905
NF3			1.000	0.000	1.000
Training dataset	0.908	0.092	0.938	0.062	0.930
Validation dataset	0.939	0.061	0.881	0.119	0.897

**TABLE 4. Performance comparison of the models at sample granularity on the validation dataset.**

Model	TPR	FNR	TNR	FPR	ACC
FSM	0.939	0.061	0.881	0.119	0.897
SVM-1	0.710	0.290	0.910	0.090	0.856
SVM-2	0.682	0.318	0.929	0.071	0.862
SVM-4	0.700	0.300	0.931	0.069	0.868
SVM-8	0.771	0.229	0.916	0.084	0.877
SVM-16	0.764	0.236	0.918	0.082	0.876
SVM-32	0.708	0.292	0.924	0.076	0.865
SVM-64	0.648	0.352	0.922	0.078	0.847
SVM-128	0.632	0.368	0.933	0.067	0.850
ANN-1	0.648	0.352	0.928	0.072	0.852
ANN-2	0.744	0.256	0.946	0.054	0.891
ANN-4	0.643	0.357	0.963	0.037	0.876
ANN-8	0.756	0.244	0.946	0.054	0.894
ANN-16	0.777	0.223	0.919	0.081	0.880

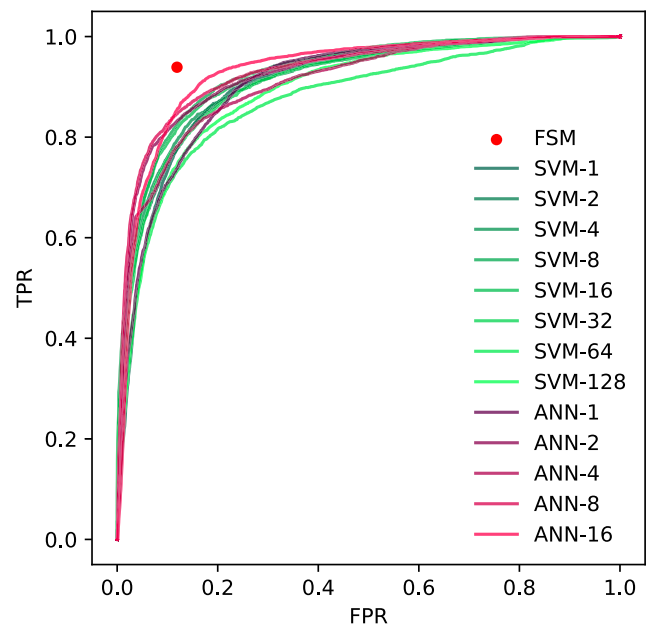


**FIGURE 5. FSM and SVM models compared against the ANN ROC curve of the ANN.**

increase either the TPR or the TNR, we generated a ROC curve (Figure 5).

In terms of TPR, TNR and accuracy, the FSM exhibited better performance than the SVM and ANN model. However

**TABLE 5.** Performance comparison of the models.

Model	Performance (Hz)
FSM	9,974 Hz
SVN-1	3,428 Hz
SVN-2	2,761 Hz
SVN-4	1,907 Hz
SVN-8	847 Hz
SVN-16	393 Hz
SVN-32	178 Hz
SVN-64	75 Hz
SVN-128	32 Hz
ANN-1	10,919,943 Hz
ANN-2	4,607,538 Hz
ANN-4	1,732,995 Hz
ANN-8	579,057 Hz
ANN-16	158,399 Hz

these results must be interpreted with caution, as the validation dataset may have affected differently the training of both the FSM and the ANN, introducing biases that could potentially skew the model comparison between the models. Moreover, the SVM models were not exposed to validation during training, ensuring they remained unbiased by the validation/testing dataset. This disadvantaged the SVM models compared to the other models. Additionally, it is also arguable that these performance results may not necessarily reflect the performance at the more relevant event granularity.

In addition to classification performance, model speed is another essential factor to consider when selecting a model. To evaluate the computational performance of the models, we processed the entire datasets with each model and measured how many LIDAR frames they could process per second on an Intel Core i7-13700KF<sup>5</sup> (Table 5).

The findings indicated that the FSM outperformed the SVM models in computational efficiency, yet it was outpaced by the ANN models. Given that the SVM and ANN models leverage the highly optimized scikit-learn and PyTorch libraries, coded in lower-level languages like C or C++, and considering the FSM model was developed solely in Python, it is anticipated that the performance of the FSM could significantly improve if the algorithm were reimplemented in a lower-level language.

To evaluate the FSM's computing performance on lower-power devices, we executed it on a Raspberry Pi 3 single board computer (SBC) and achieved a performance of 340 Hz. These findings indicate that if the algorithm were implemented in C on a microcontroller with approximately 100 MHz processing power, it would likely exceed the acquisition rate of 10 Hz.

## V. DISCUSSION

One of the main advantages of our FSM approach is its clarity and direct grounding in the knowledge of fall phenomena. Unlike other black-box methods, such as machine learning-based algorithms, our system allows for a clear and logical

<sup>5</sup><https://www.intel.com/content/www/us/en/products/sku/230489/intel-core-i713700kf-processor-30m-cache-up-to-5-40-ghz/specifications.html>

understanding of each decision made. This is especially valuable in cases of failure, where the cause of the problem can be understood and effectively addressed.

A significant limitation of the ST VL53L5CX is its narrow FOV of 45° x 45°, which restricts its ability to cover a substantial physical area, to the extent that falls may not entirely occur within its FOV. One approach to overcome this limitation is to employ LIDARs with a broader FOV, like the ST VL53L7CH and ST VL53L7CX, which offer a 60° x 60° FOV. However, these LIDARs have a shorter range and face challenges in measuring light reflected from dark, opaque surfaces. Alternatively, increasing coverage can be achieved by using multiple LIDARs, taking advantage of their cost-effectiveness (approximately \$6 at the time of writing).

An important consideration to implement fall detection is the ratio between FN and FP. Both situations reduce the accuracy of the algorithm, but a FN can imply a undetected fall that is serious enough to require immediate attention, while a FP represents only a false alarm. The probability output of the ANN and SVM make these models easy to tweak to through their probability output to prioritize either reduction of FNs or FPs. On the contrary, adjusting the FSM model involves modifying the objective function of the optimizer to alter the penalties associated with FNs and FPs.

It is important to highlight that the limited availability of a larger subject pool made it challenging to evaluate the models. The insufficient number of subjects hindered the creation of a testing dataset without significantly compromising the training and validation of the models. Despite this, this paper provides preliminary results on the performance that could be expected from different LIDAR-based fall detection algorithms.

Our FSM model's simplicity and effectiveness, as evidenced by its classification performance, position it as an optimal choice for deployment on inexpensive microcontrollers. This, in turn, could facilitate the deployment of multiple units in elderly household settings without increasing costs prohibitively high.

## VI. CONCLUSION

In this work, a fall detection system based on a LIDAR sensor was presented, emphasizing its low-cost, respect for privacy, and non-intrusive character. By avoiding cameras and other intrusive or wearable devices, we not only ensure the protection of user privacy, but also prevent any alteration in the daily routines of the elderly. These aspects are very relevant in order not to compromise the quality and well-being in the usual living environment of the elderly.

This work can be considered as an initial step in the ongoing development of a system designed to monitor and analyze a broader spectrum of daily activities and behaviors. This expansion may involve the identification of atypical movement patterns or early detection of conditions that could potentially result in falls or other health-related incidents. Furthermore, the integration of a LIDAR with various other sensor, such as biometric or environmental sensors, has the

potential to enhance the detection capabilities of the system, which could enable a more thorough analysis to cater to the diverse needs of users.

In a practical scenario, deploying multiple LIDAR units becomes essential for full room coverage. This setup would not just improve the ability to detect falls on a wider area, but it would also significantly enhance the system's ability to pinpoint unusual activity. While each LIDAR unit could operate independently with its own FSM, integrating multiple units could greatly increase the detection capability of the system.

It is also worth noting that adjustments made under controlled conditions may not necessarily translate to real-world effectiveness. Thus, the system can refine its detection capabilities in new environments by leveraging techniques like universal source-free domain adaptation or online learning. This approach involves initial learning in controlled settings followed by automatic fine-tuning to adapt to the specific conditions of each home, thereby enhancing the system's precision and real-time effectiveness.

We believe this work is just the beginning of further developing the system to monitor and analyze a wider range of everyday activities and behaviors. This could include identifying unusual movement patterns or early detection of conditions that might lead to falls or other health incidents. Moreover, combining LIDAR with diverse sensors, including biometric and environmental sensors, holds the potential to augment the system's detection capabilities. This enhancement could facilitate a more comprehensive analysis, addressing the varied needs of users more effectively.

## ACKNOWLEDGMENT

The authors would like to thank ANID—MILENIO—NCS2021\_013.

## REFERENCES

- [1] *World Population Prospects 2022: Summary of Results*, 2022.
- [2] C. Taramasco, T. Rodenas, F. Martinez, P. Fuentes, R. Munoz, R. Olivares, V. H. C. De Albuquerque, and J. Demongeot, "A novel monitoring system for fall detection in older people," *IEEE Access*, vol. 6, pp. 43563–43574, 2018.
- [3] Statista. (1950). *Total Fertility Rate Globally and By Continent 1950-2024*. [Online]. Available: <https://www.statista.com/statistics/1034075/fertility-rate-world-continents-1950-2020/>
- [4] L. Palmerini, J. Klenk, C. Becker, and L. Chiari, "Accelerometer-based fall detection using machine learning: Training and testing on real-world falls," *Sensors*, vol. 20, no. 22, p. 6479, Nov. 2020.
- [5] B. Pandya, A. Pourabdollah, and A. Lotfi, "Comparative analysis of real-time fall detection using fuzzy logic Web services and machine learning," *Technologies*, vol. 8, no. 4, p. 74, Dec. 2020.
- [6] S. Hellmers, E. Krey, A. Gashi, J. Koschate, L. Schmidt, T. Stuckenschneider, A. Hein, and T. Zieschang, "Comparison of machine learning approaches for near-fall-detection with motion sensors," *Frontiers Digit. Health*, vol. 5, pp. 1–12, Jul. 2023.
- [7] A. Chelli and M. Pätzold, "A machine learning approach for fall detection and daily living activity recognition," *IEEE Access*, vol. 7, pp. 38670–38687, 2019.
- [8] S. Wang, F. Miranda, Y. Wang, R. Rasheed, and T. Bhatt, "Near-fall detection in unexpected slips during over-ground locomotion with body-worn sensors among older adults," *Sensors*, vol. 22, no. 9, p. 3334, Apr. 2022.
- [9] M. E. N. Gomes, D. Macêdo, C. Zanchettin, P. S. G. de-Mattos-Neto, and A. Oliveira, "Multi-human fall detection and localization in videos," *Comput. Vis. Image Understand.*, vol. 220, Jul. 2022, Art. no. 103442.
- [10] M. Salimi, J. J. M. Machado, and J. M. R. S. Tavares, "Using deep neural networks for human fall detection based on pose estimation," *Sensors*, vol. 22, no. 12, p. 4544, Jun. 2022.
- [11] R. Egawa, A. S. M. Miah, K. Hirooka, Y. Tomioka, and J. Shin, "Dynamic fall detection using graph-based spatial temporal convolution and attention network," *Electronics*, vol. 12, no. 15, p. 3234, Jul. 2023.
- [12] C.-B. Lin, Z. Dong, W.-K. Kuan, and Y.-F. Huang, "A framework for fall detection based on OpenPose skeleton and LSTM/GRU models," *Appl. Sci.*, vol. 11, no. 1, p. 329, Dec. 2020.
- [13] Y. Shao, X. Wang, W. Song, S. Ilyas, H. Guo, and W.-S. Chang, "Feasibility of using floor vibration to detect human falls," *Int. J. Environ. Res. Public Health*, vol. 18, no. 1, p. 200, Dec. 2020.
- [14] I. Cho, I. S. Jin, H. Park, and P. C. Dykes, "Clinical impact of an analytic tool for predicting the fall risk in inpatients: Controlled interrupted time series," *JMIR Med. Informat.*, vol. 9, no. 11, Nov. 2021, Art. no. e26456.
- [15] I. Bargiotas, D. Wang, J. Mantilla, F. Quijoux, A. Moreau, C. Vidal, R. Barrois, A. Nicolai, J. Audiffren, C. Labourdet, F. Bertin-Hugaul, L. Oudre, S. Buffat, A. Yelnik, D. Ricard, N. Vayatis, and P.-P. Vidal, "Preventing falls: The use of machine learning for the prediction of future falls in individuals without history of fall," *J. Neurol.*, vol. 270, no. 2, pp. 618–631, Feb. 2023.
- [16] S. Usmani, A. Saboor, M. Haris, M. A. Khan, and H. Park, "Latest research trends in fall detection and prevention using machine learning: A systematic review," *Sensors*, vol. 21, no. 15, p. 5134, Jul. 2021.
- [17] G. Márquez, A. Veloz, J.-G. Minoz, C. Reyes, E. Calvo, and C. Taramasco, "Using low-resolution non-invasive infrared sensors to classify activities and falls in older adults," *Sensors*, vol. 22, no. 6, p. 2321, Mar. 2022.
- [18] P. V. Er and K. K. Tan, "Non-intrusive fall detection monitoring for the elderly based on fuzzy logic," *Measurement*, vol. 124, pp. 91–102, Aug. 2018.
- [19] F. Riquelme, C. Espinoza, T. Rodenas, J.-G. Minoz, and C. Taramasco, "EHomeSeniors dataset: An infrared thermal sensor dataset for automatic fall detection research," *Sensors*, vol. 19, no. 20, p. 4565, Oct. 2019.
- [20] N. T. Pro. *Why Are Thermal Cameras So Expensive? an Ultimate Guide to Thermal Imagers*. Accessed: Apr. 17, 2024. [Online]. Available: <https://novatestpro.com/pages/why-are-thermal-imaging-cameras-so-expensive>
- [21] M. Ghassemi, T. Naumann, P. Schulam, A. L. Beam, I. Y. Chen, and R. Ranganath, "A review of challenges and opportunities in machine learning for health," *AMIA Summits Transl. Sci. Proc.*, vol. 2020, pp. 191–200, May 2020.
- [22] L. Gao and L. Guan, "Interpretability of machine learning: Recent advances and future prospects," *IEEE MultimediaMag.*, pp. 1–12, 2023.
- [23] M. Fañez, J. R. Villar, E. de la Cal, V. M. González, J. Sedano, and S. B. Khojasteh, "Mixing user-centered and generalized models for fall detection," *Neurocomputing*, vol. 452, pp. 473–486, Sep. 2021.
- [24] F. Hussain, F. Hussain, M. Ehatisham-ul-Haq, and M. A. Azam, "Activity-aware fall detection and recognition based on wearable sensors," *IEEE Sensors J.*, vol. 19, no. 12, pp. 4528–4536, Jun. 2019.
- [25] N. Frøvik, B. A. Malekzai, and K. Øvsthus, "Utilising LiDAR for fall detection," *Healthcare Technol. Lett.*, vol. 8, no. 1, pp. 11–17, Feb. 2021.
- [26] D. Hutabarat, M. Rivai, D. Purwanto, and H. Hutomo, "LiDAR-based obstacle avoidance for the autonomous mobile robot," in *Proc. 12th Int. Conf. Inf. Commun. Technol. Syst. (ICTS)*, Jul. 2019, pp. 197–202.
- [27] V. Molebny, P. Mcmanamon, O. Steinvall, T. Kobayashi, and W. Chen, "Laser radar: Historical perspective—From the east to the west," *Opt. Eng.*, vol. 56, no. 3, Dec. 2016, Art. no. 031220, doi: 10.1117/1.oe.56.3.031220.
- [28] J. Wagner, P. Mazurek, A. Miekina, R. Z. Morawski, F. F. Jacobsen, T. T. Sudmann, I. T. Børsheim, K. Øvsthus, and T. Ciamulski, "Comparison of two techniques for monitoring of human movements," *Measurement*, vol. 111, pp. 420–431, Dec. 2017.
- [29] D. Asbjørn and T. Jim, "Recognizing bedside events using thermal and ultrasonic readings," *Sensors*, vol. 17, no. 6, p. 1342, Jun. 2017.
- [30] E. Ackerman, "LiDAR that will make self-driving cars affordable [News]," *IEEE Spectr.*, vol. 53, no. 10, pp. 1–14, Oct. 2016.
- [31] C. V. Poulton, A. Yaacobi, D. B. Cole, M. J. Byrd, M. Raval, D. Vermeulen, and M. R. Watts, "Coherent solid-state LiDAR with silicon photonic optical phased arrays," *Opt. Lett.*, vol. 42, no. 20, p. 4091, Oct. 2017.

- [32] S. Yamada, H. Rizk, and H. Yamaguchi, "An accurate point cloud-based human identification using micro-size LiDAR," in *Proc. IEEE Int. Conf. Pervas. Comput. Commun. Workshops other Affiliated Events*, Mar. 2022, pp. 569–574.
- [33] R. Ukyo, T. Amano, H. Rizk, and H. Yamaguchi, "Pedestrian tracking using 3D LiDAR—Case for proximity scenario," in *Proc. IEEE 26th Int. Conf. Intell. Transp. Syst.*, Jul. 2023, pp. 4683–4689.
- [34] M. Ohno, R. Ukyo, T. Amano, H. Rizk, and H. Yamaguchi, "Privacy-preserving pedestrian tracking using distributed 3D LiDARs," in *Proc. IEEE Int. Conf. Pervasive Comput. Commun.*, Mar. 2023, pp. 43–52.
- [35] H. Rizk, Y. Okochi, and H. Yamaguchi, "Demonstrating hitonavi-u: A novel wearable LiDAR for human activity recognition," in *Proc. 28th Annu. Int. Conf. Mobile Comput. Netw.*, New York, NY, USA: Association for Computing Machinery, Oct. 2022, pp. 756–757, doi: 10.1145/3495243.3558744.
- [36] M. Bouazizi, A. L. Mora, K. Feghouli, and T. Ohtsuki, "Activity detection in indoor environments using multiple 2D LiDARs," *Sensors*, vol. 24, no. 2, p. 626, Jan. 2024.
- [37] S. Yamada, H. Rizk, T. Amano, and H. Yamaguchi, "Fall detection and assessment using multitask learning and micro-sized LiDAR in elderly care," vol. 11, 2023.
- [38] W. Wijayanti, H. Miawarni, N. E. B. N. E. Budiayanta, D. A. Rivai, and M. H. Purnomo, "Fall detection system for elderly activity daily living using modified 2D LiDAR as a low-cost alternative to 3D LiDAR based on the slice feature approach," *Int. J. Electr. Eng. Informat.*, vol. 15, no. 2, pp. 291–304, Jun. 2023.
- [39] J. Gutiérrez, V. Rodríguez, and S. Martín, "Comprehensive review of vision-based fall detection systems," *Sensors*, vol. 21, no. 3, p. 947, Feb. 2021.
- [40] N. T. Newaz and E. Hanada, "The methods of fall detection: A literature review," *Sensors*, vol. 23, no. 11, p. 5212, May 2023.
- [41] Z. Rahemtulla, A. Turner, C. Oliveira, J. Kaner, T. Dias, and T. Hughes-Riley, "The design and engineering of a fall and near-fall detection electronic textile," *Materials*, vol. 16, no. 5, p. 1920, Feb. 2023.
- [42] V. Roshdibenam, G. J. Jogerst, N. R. Butler, and S. Baek, "Machine learning prediction of fall risk in older adults using timed up and go test kinematics," *Sensors*, vol. 21, no. 10, p. 3481, May 2021.
- [43] J. R. Villar, C. Chira, E. de la Cal, V. M. González, J. Sedano, and S. B. Khojasteh, "Autonomous on-wrist acceleration-based fall detection systems: Unsolved challenges," *Neurocomputing*, vol. 452, pp. 404–413, Sep. 2021.
- [44] A. Shahzad and K. Kim, "FallDroid: An automated smart-phone-based fall detection system using multiple kernel learning," *IEEE Trans. Ind. Informat.*, vol. 15, no. 1, pp. 35–44, Jan. 2019.
- [45] A. Sixsmith and N. Johnson, "A smart sensor to detect the falls of the elderly," *IEEE Pervas. Comput.*, vol. 3, no. 2, pp. 42–47, Apr. 2004.
- [46] Y. Taniguchi, H. Nakajima, N. Tsuchiya, J. Tanaka, F. Aita, and Y. Hata, "A falling detection system with plural thermal array sensors," in *Proc. Joint 7th Int. Conf. Soft Comput. Intell. Syst. (SCIS) 15th Int. Symp. Adv. Intell. Syst. (ISIS)*, Dec. 2014, pp. 673–678.
- [47] X. Fan, H. Zhang, C. Leung, and Z. Shen, "Robust unobtrusive fall detection using infrared array sensors," in *Proc. IEEE Int. Conf. Multisensor Fusion Integr. Intell. Syst. (MFI)*, Nov. 2017, pp. 194–199.
- [48] Y. Chu, K. Cumanan, S. K. Sankarpani, S. Smith, and O. A. Dobre, "Deep learning-based fall detection using WiFi channel state information," *IEEE Access*, vol. 11, pp. 83763–83780, 2023.
- [49] A. Rezaei, A. Mascheroni, M. C. Stevens, R. Argha, M. Papandrea, A. Puiatti, and N. H. Lovell, "Unobtrusive human fall detection system using mmWave radar and data driven methods," *IEEE Sensors J.*, vol. 23, no. 7, pp. 7968–7976, Apr. 2023.



**DAVID ARAYA** received the B.Sc. and P.E. degrees in electrical engineering from the Universidad de Chile, in 2005. He is currently pursuing the Ph.D. degree in science with a mention in biophysics and computational biology with the Universidad de Valparaíso. He is currently a Professor and a Researcher with the Universidad Andrés Bello, with extensive knowledge in AI and neuroscience. His expertise at the intersection of these disciplines enables him to address complex issues related to human brain function. His Ph.D. research was dedicated to the early detection of psychiatric disorders through brain markers. Beyond neuroscience, he has explored how AI can drive the development of innovative health technologies. Currently, he applies his deep understanding of AI and computational neuroscience with the Institute of Technology and Innovation for Health and Wellbeing (ITISB), leading research and development projects that aim to advance healthcare technologies.



**DAVID RUETE** received the master's and Ph.D. degrees in multimedia technologies. He is currently an Associate Professor with the Faculty of Engineering, Andrés Bello University. He has authored over 30 scientific papers in refereed international conferences and journals. His research interests include machine learning, AI, higher-order thinking skills, education, and educational management.



**CARLA TARAMASCO** received the B.Eng. degree in computer engineering from the Universidad de Valparaso, Chile, in 2001, the M.Sc. degree in cognitive science from the École Normale Supérieure, in 2006, and the Ph.D. degree (summa cum laude) from the École Polytechnique, France, in 2011. She is currently a Full Professor with the Faculty of Engineering, Andrés Bello University, and the Director of the Institute of Technology for Innovation in Health and Wellbeing (ITISB). She is also a member of the Executive Committee of the National Centre for Health Information Systems. She has scientific publications in books, journals, and conference proceedings. She has organized over 20 international workshops/sessions and has acted as a coordinator for over 40 national and international projects. She was involved in the development of networks for scientific collaboration between Africa, South America, and Europe. She has involved in the investigation and development of technological solutions for health-monitoring software and hardware. Her main academic and research interests include health, which includes mHealth, ambient assisted living for older people, e-health, telemedicine and telerehabilitation, supervision of chronic diseases, and complex social systems, including dynamic networks, socio-semantic networks, and analysis of trajectories both individual and collective. She also teaches both at the undergraduate and graduate levels, along with scientific divulgation.



**MIGUEL PIÑEIRO** received the B.Sc. degree in informatics engineering from the Universidad de Viña del Mar and the Ph.D. degree in neuroscience from the Universidad de Valparaíso. He is currently with the Institute of Technology and Innovation for Health and Wellbeing (ITISB), where he has focused on pattern detection of sensor data and design of hardware devices.